

Apollo 17

DEVELOPMENT OF THE APOLLO MISSION 17 CONTROL NETWORK

For The  
NATIONAL AERONAUTICS AND SPACE ADMINISTRATION  
Under  
Contract No. W-13,408

January 1975

Prepared By  
Defense Mapping Agency Aerospace Center  
Department of Defense  
St. Louis AFS, Mo. 63118

## TABLE OF CONTENTS

	<u>Page</u>
List of Figures	i
List of Tables	ii
1. Introduction	1
1.1 Background	1
1.2 Initial Photographic Evaluation	1
2. Apollo Mission 17 Reduction Plan	1
3. Stellar Derived Orientations	2
3.1 Camera Calibration	2
3.2 Identification and Mensuration	5
3.3 Reduction Processing	5
3.4 Analysis of Results	7
4. Image Coordinate Acquisition and Reduction	14
4.1 Identification and Mensuration	14
4.2 Image Coordinate Reduction	15
4.2.1 Correction for Forward Motion Compensation	15
4.2.2 Correction for Systematic Errors	15
4.3 Altimeter Image Coordinates	16
5. Analytical Triangulation	16
5.1 Strip Relative Solutions	16
5.2 Strip Constrained Solutions	18
5.3 Block Triangulation Solution	22
6. Positional Evaluation	28
6.1 Relative Accuracy of Coordinates	28
6.2 Relative Position of Apollo Mission 17 and Apollo Mission 15 Solutions	31
6.3 Laser Altimeter Slant Range Derivation	31
6.4 Absolute Positional Evaluation	31

## LIST OF FIGURES

<u>Figure Number</u>	<u>Title</u>	<u>Page</u>
1	Limits of Selected Metric Camera System Coverage	4
2	Stellar Plate Residuals Before and After Removal of Decentering Distortion	6
3	First Differences in Mapping Camera Orientation Angles	8
3.1	First Differences in Mapping Camera Orientation Angles	9
3.2	First Differences in Mapping Camera Orientation Angles	10
3.3	First Differences in Mapping Camera Orientation Angles	11
3.4	First Differences in Mapping Camera Orientation Angles	12
3.5	First Differences in Mapping Camera Orientation Angles	13
4	Horizontal Adjustment of Strip SAPGO Solution	19
4.1	Vertical Adjustment of Strip SAPGO Solution	20
4.2	Horizontal and Vertical Adjustments of Strip SAPGO Solutions	21
5	Horizontal Change to Camera Positions Final Block Solution	25
5.1	Vertical Change to Camera Positions Final Block Solution	26
6	Common Vertical Photographic Coverage Between Apollo Missions 15 and 17	27
7	Horizontal Position Comparison of Apollo 17 to the Apollo 15 Block Solution	33
7.1	Vertical Position Comparison of Apollo 17 to the Apollo 15 Block Solution	34

	<u>Page</u>
7. Generated Products	35
8. Conclusions	36
References	37
Appendix A - Camera Calibration Summary	A1
Appendix B - Inertial Measurement Unit Minus Stellar Reduction	B1
Appendix C - Unique Numbering Scheme	C1

## LIST OF TABLES

<u>Table Number</u>	<u>Title</u>	<u>Page</u>
1	Photographs Selected for Data Reduction	3
2	Exposures with Derived Altimeter Slant Range	17
3	Mean Systematic Biases Between Common Surface Coordinates Derived in Independent Strip Sappo Solutions	23
4	Standard Deviations Computed from Comparisons of Coordinates Common to Two or More Strips	29
5	Estimated Accuracy Between Points Separated by Various Distances	32

## 1. Introduction

### 1.1 Background

Triangulation efforts using Metric Camera System near vertical photography began in 1971 with the acquisition of Apollo Mission 15 materials. Within the Defense Mapping Agency, subsequent assignments were made as Apollo Mission 16 and 17 were completed. With the return of the photographic materials from the Apollo Mission 17, the National Aeronautics and Space Administration (NASA) initiated a data reduction assignment of Apollo 17 which would contribute to the unified selenodetic network. The Apollo 17 near vertical photography covers approximately 3,915,000 sq. km. extending 247° from 155° W. to 42° W. This data reduction was accomplished for NASA by the Defense Mapping Agency Aerospace Center (DMAAC).

In addition to the photogrammetric data generation and solutions contained in the DMAAC Apollo 17 Metric Camera System Data Reduction proposal, two reports were to be prepared during the project. The first was to address an initial evaluation of the Apollo 17 photographic system and the second was to document the results of the completed reduction. The initial report, entitled "Apollo 17 Metric System, Initial Evaluation Report," was completed and released in April 1974. (1) The following pages document the results of the second report and contain a description of the overall plan for the Apollo 17 reduction, the results of the stellar orientation and mapping camera measurement phases, the analytical triangulation solutions, and the positional evaluation of the developed selenographic coordinates.

### 1.2 Initial Photographic Evaluation

The primary purpose of the initial test was to evaluate the Apollo Mission 17 photographic system. The reader should refer to the Initial Test Report for a detailed description of techniques or procedures. Changes to techniques used in the Initial Test were made for some operations to increase accuracy or production efficiency. These changes are noted in the text and the procedure actually used is explained.

## 2. Apollo Mission 17 Reduction Plan

All or parts of 8 revolutions were reduced to provide comprehensive Apollo Mission 17 coverage of the moon's surface, provide an evaluation of the ephemeris positions, and to supplement the area covered by Apollo Mission 15.

The even numbered photographs, which provided 56 percent forward overlap, were used as a cost effective method of deriving lunar surface positions. Exceptions to the criterion of 56 percent forward overlap between alternate photographs were encountered when changes in the spacecraft altitude resulted in changes in the photographic scale. To maintain this desired overlap every photograph was used from exposure 180 through 232 and exposures 1821 and 1825 and every third photograph from exposure 276 through 303. Every photograph between exposure 232 through 256 and 2030 through 2050 was used because the blurred image of a lens cover obscured part of lunar imagery. The final coverage selection resulted in the use of 408 terrain photographs. The side overlap between adjacent revolutions ranged from 10 to 95 percent. Table 1 lists the selected photographs and Figure 1 shows the area of coverage.

The Apollo 17 reduction was planned by revolutions (strips) and the general procedure was as follows:

- A. Stellar reductions were performed on a strip basis.
- B. Selected point and image measurements were made on photographs of each strip. (Points identified on Apollo 15 photography would be used, if practical.)
- C. Quality control checks on the data from each revolution were made using the Rigorous Analytical Block Orientation (RABO) Program.
- D. Strip solutions were performed using the Simultaneous Adjustment of Photogrammetric and Geodetic Observations (SAPGO) Program.
- E. Common points were evaluated in side-lap areas.
- F. Assembled strips in an Analytical (SAPGO) Block Solution.
- G. Accomplished an analytical triangulation with data from the adjusted block.

The following sections of the report give a more detailed account of each step in the procedure.

### 3. Stellar Derived Orientations

#### 3.1 Camera Calibration

In the initial evaluation of the Apollo 17 Metric System unusually large systematic x residuals were noted in the stellar

TABLE 1

PHOTOGRAPHS SELECTED FOR DATA REDUCTION

<u>Revolution</u>	<u>Vertical Exposure</u>	<u>Stellar Exposure</u>
2	170-180 181-256* 258-276 279-306**	152-162 163-213*
14	328-430	318-412
29	1384-1480	1372-1462
38	1692-1820 1821,1822 1824,1825 1826,1828	1682-1802 1803,1804 1806,1807 1808,1810
49	2030-2050*	
62	2200-2220	2182-2202
66	2630-2660 2700-2732	2612-2642 2682-2714
74	2796-2932	2786-2914

Even numbered exposures were used unless noted

\* Every exposure used

\*\* Every third exposure used



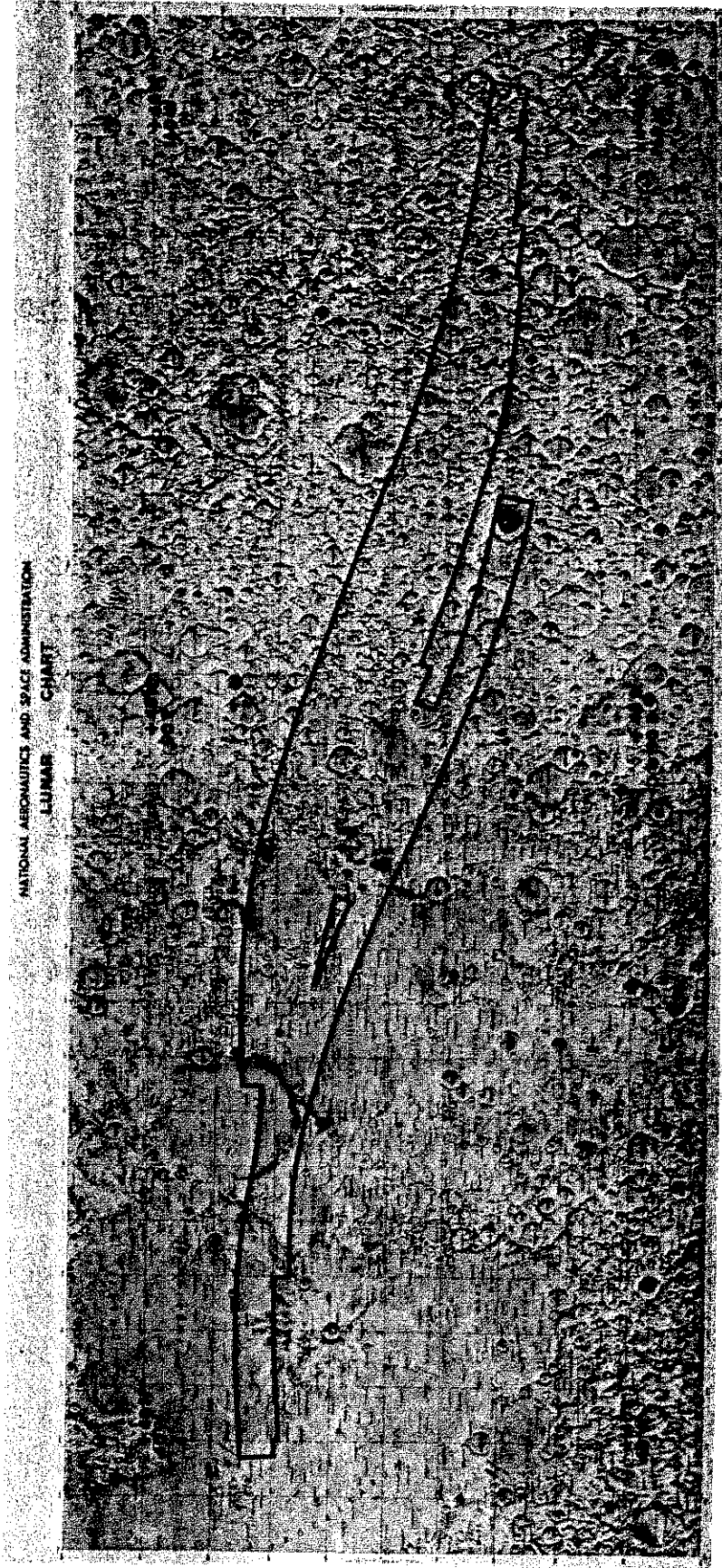


FIGURE 1. LIMITS OF SELECTED METRIC CAMERA SYSTEM COVERAGE.

orientation reductions. The standard deviations developed in the Stellar Attitude for a Lunar Mapping Camera (SATLUM) (2) Program for the mapping camera orientations were approximately twice those experienced with Apollo Mission 15 stellar reductions. The photo-coordinate residuals exhibited an anomaly in the X component; the average X residual standard deviation (6.4  $\mu\text{m}$ ) being approximately two times as large as the average Y residual standard deviation (3.7  $\mu\text{m}$ ). This residual pattern was identified as lens decentering distortion and NASA was notified of the problem. NASA authorized DMAAC to perform a calibration of the Lunar Mapping Camera Unit SN-004 using the original preflight calibration materials and supporting data. The results of this calibration, published by DMAAC in June 1974 (3), were used in the reduction of the Apollo 17 photographs. Figure 2 shows an example of the change in the X residual pattern by removing the decentering distortion. A summary of the DMAAC calibration is given in Appendix A.

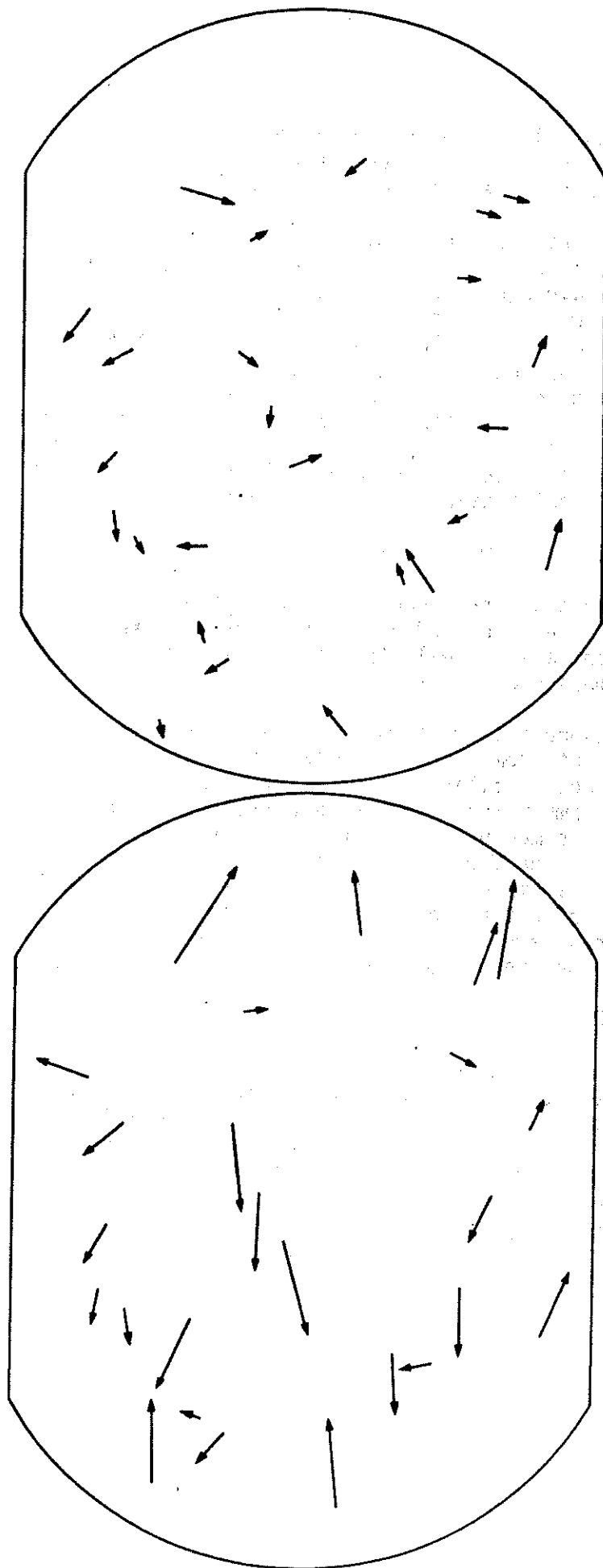
### 3.2 Identification and Mensuration

Each stellar photograph contained approximately 25 well distributed stars. For each of 332 of the 408 terrain exposures used in the reduction, a companion stellar photograph was measured. Table 1 lists the exposures measured.

Stellar measurements were made on third generation film positives which were cut from a roll by DMAAC into five exposure segments for convenience in filing and measuring. Mensuration was done on a Mann monoscopic comparator with each measure punched on a separate card. Each exposure was measured twice with the second set of measurements rotated 180° from the first. All reseau marks on a stellar photograph were measured in a standard sequence. Stars images were then measured with the aid of a transparent template made from a star chart. These "normal" readings were repeated in the "reverse" sense (photograph rotated 180°) for the second set of readings.

### 3.3 Reduction Processing

The Stellar Attitude for a Lunar Mapping Camera (SATLUM) Program, used for the Apollo 17 stellar reductions, was developed by the Raytheon Corporation. Several preprocessor type additions to the SATLUM Program were made at DMAAC in order to facilitate the simultaneous input of comparator coordinates for both the "normal" and "reverse" measurements and to accommodate small differences in the output format of different digitizers associated with the Mann comparators. Certain SATLUM output statements were also revised to conform to DMAAC formats. The star measurements for all exposures were processed with SATLUM to



RESIDUAL SCALE

0 5 10

MICROMETERS

BEFORE

AFTER

FIGURE 2. STELLAR PLATE RESIDUALS BEFORE AND AFTER REMOVAL OF DECENTERING DISTORTION.

obtain the mapping camera orientations in the Celestial 1950 System (Inertial) and the Lunar-fixed System.

The Program also computed the standard deviations for each orientation and provided orientation and covariance matrices. The standard deviations were developed by propagating the errors of the stellar resections and the interlock angles to the mapping camera orientations. Typical standard deviations for both cameras relative to the celestial coordinate system were:

	$\sigma(\omega)$	$\sigma(\phi)$	$\sigma(\kappa)$
Stellar Camera	1"8	1"7	12"6
Mapping Camera	6"8 (Roll)	12"3 (Pitch)	3"6 (Yaw)

### 3.4 Analysis of Results

The imagery on the Apollo Mission 17 stellar exposures was not as well defined as the stellar images from Apollo Mission 15. The general degradation was caused by a slight overexposure resulting from a light reflecting into the stellar camera lens. Of the 76 stellar exposures for which orientations were not developed, 65 were excessively overexposed and the remaining 11 had the stellar imagery obscured by the camera lens cap.

The stellar derived orientations were examined for consistency by plotting the first differences in the mapping camera orientation angles between alternate exposures. Figures 3 through 3.5 show the graph of the changes in the angles versus exposure numbers. Graphs of this type, for all photographic sequences, were examined as a quality control check. Departures from the normal trends in these curves were viewed as being potentially inconsistent orientation data.

The stellar orientations were also compared with the inertial measurement unit (IMU) values tabulated in the photo support data. A plot showing the differences between IMU and stellar derived orientation angles for even numbered exposures is shown in Appendix B with the delta ( $\Delta$ ) angles referenced to the stellar values. Breaks in the graphs for revolutions 14, 29 and 38 are due to incomplete IMU data. Each of the orientation elements exhibited differences of as much as 8 minutes during a revolution but with a variation about an envelope of 2 to 3 minutes. Variations in the delta angles reflect acceleration of the spacecraft to maintain a local vertical pointing of the mapping camera. The spacecraft was being maneuvered from an oblique to vertical position during revolution 62 as reflected by the radical angular changes.

# REVOLUTION 2

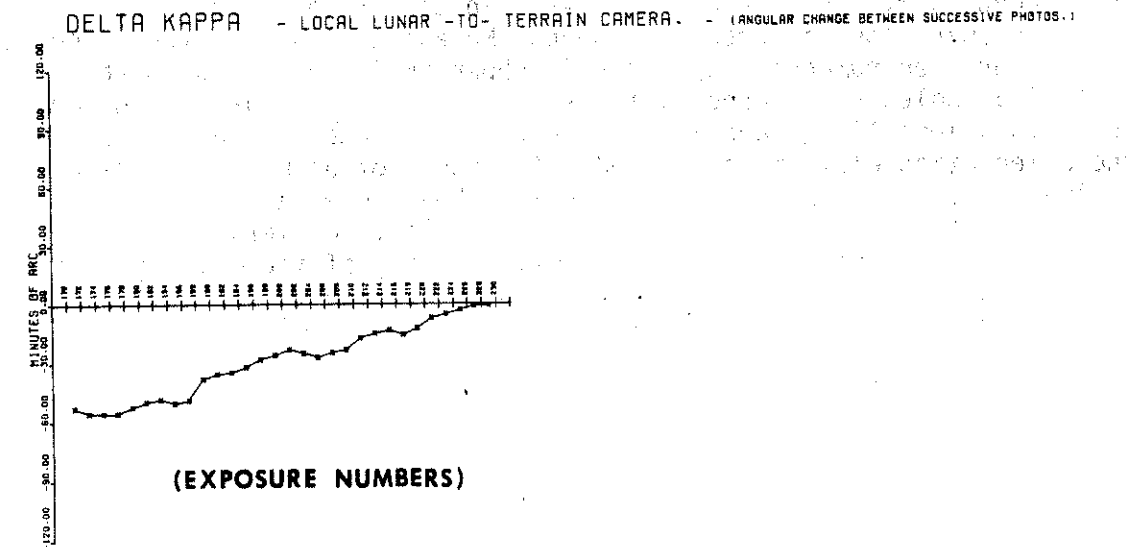
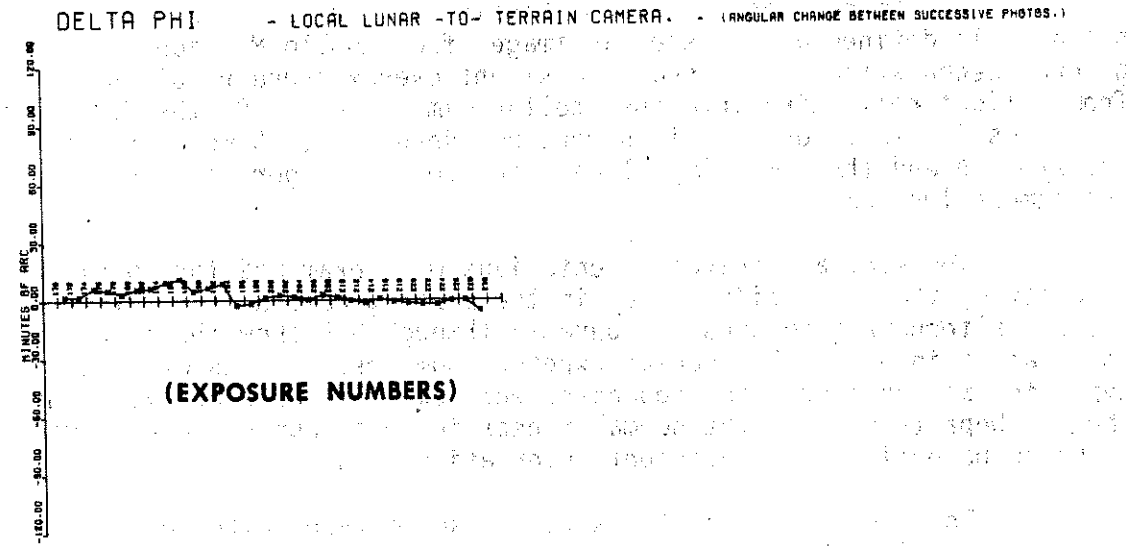
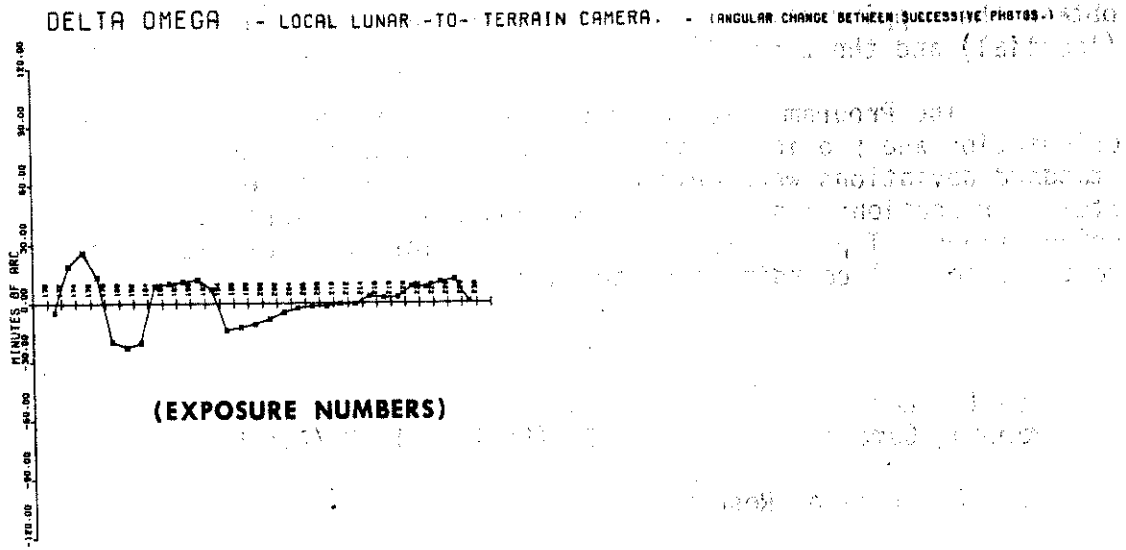


FIGURE 3. FIRST DIFFERENCES IN MAPPING CAMERA ORIENTATION ANGLES.

# REVOLUTION 14

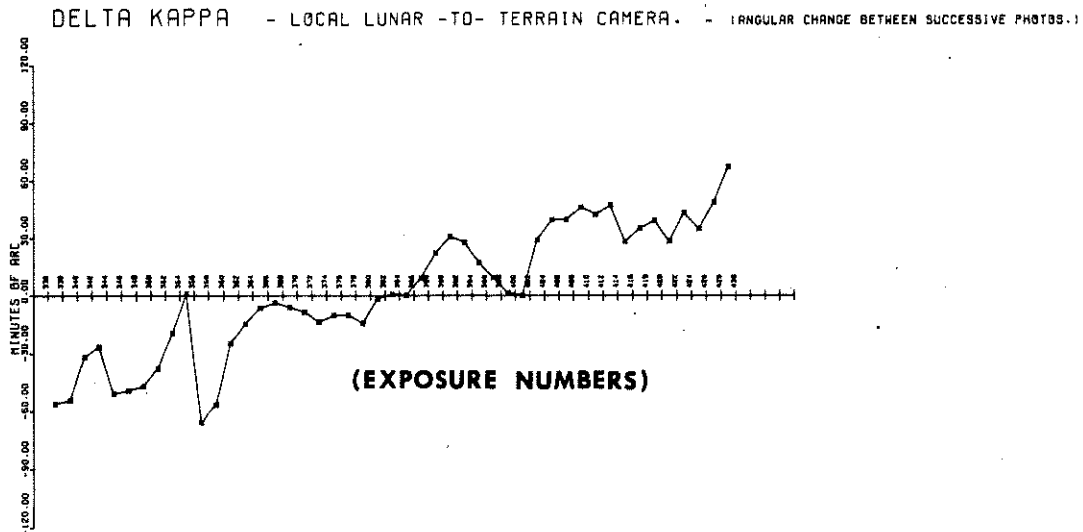
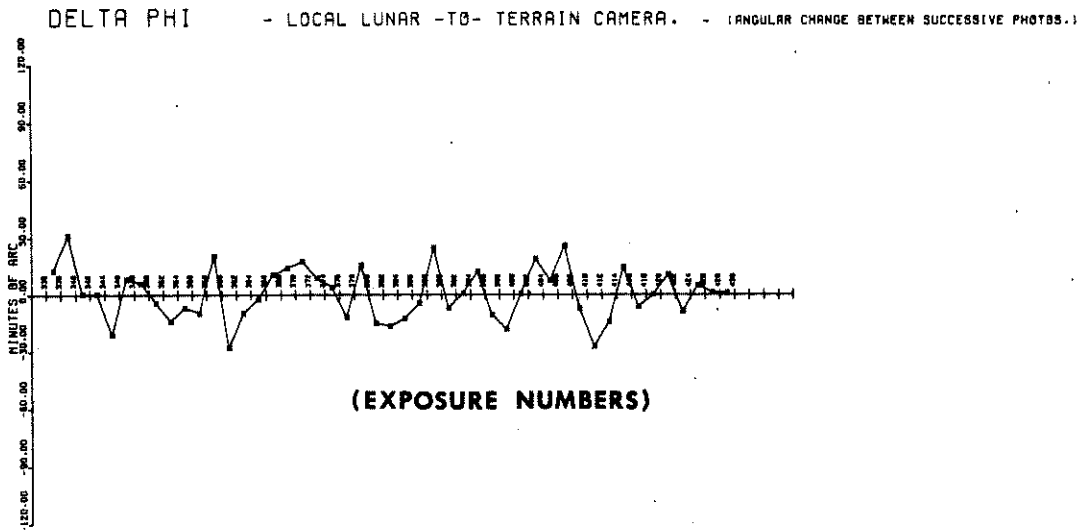
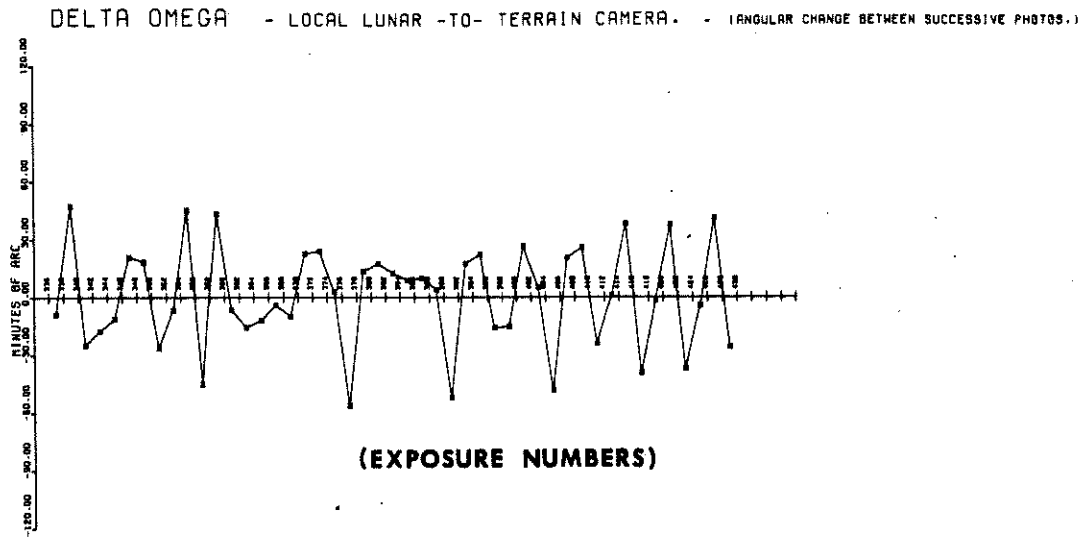


FIGURE 3.1 FIRST DIFFERENCES IN MAPPING CAMERA ORIENTATION ANGLES.

# REVOLUTION 29

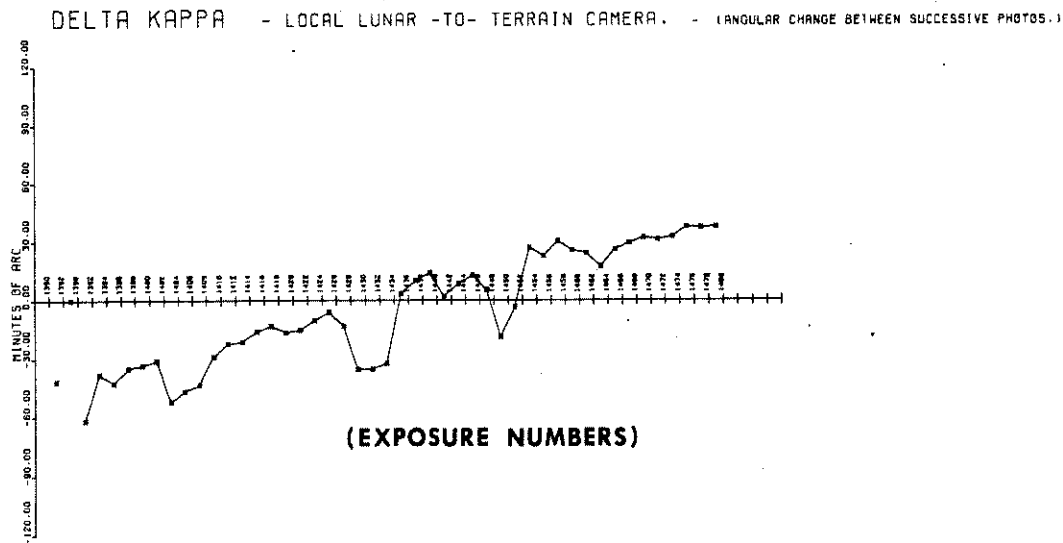
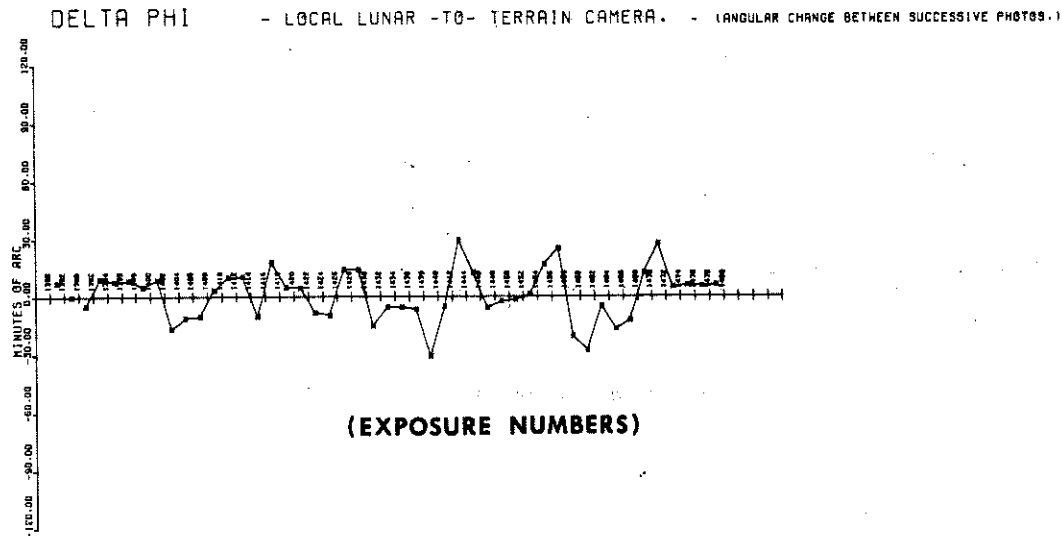
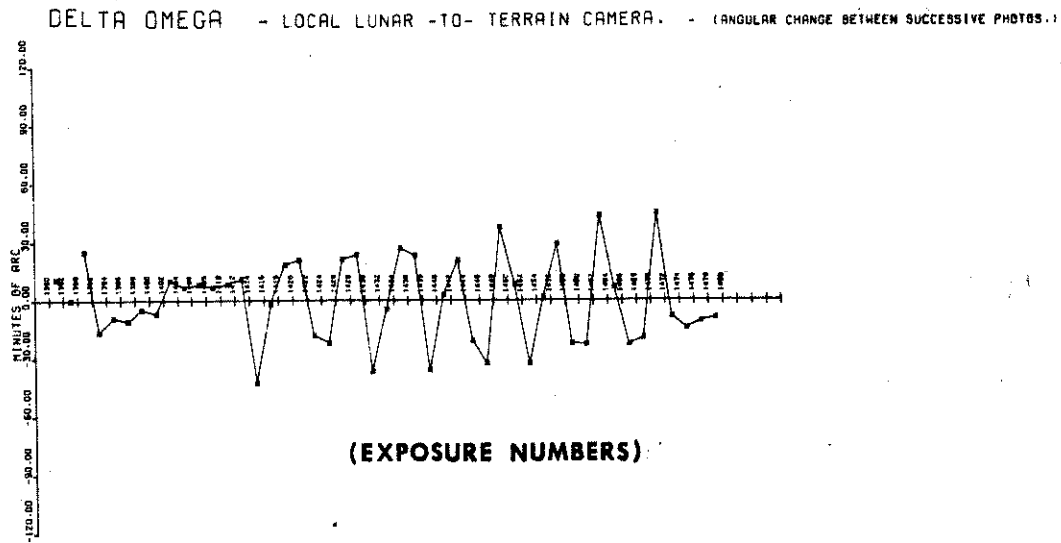


FIGURE 3.2 FIRST DIFFERENCES IN MAPPING CAMERA ORIENTATION ANGLES.

# REVOLUTION 38

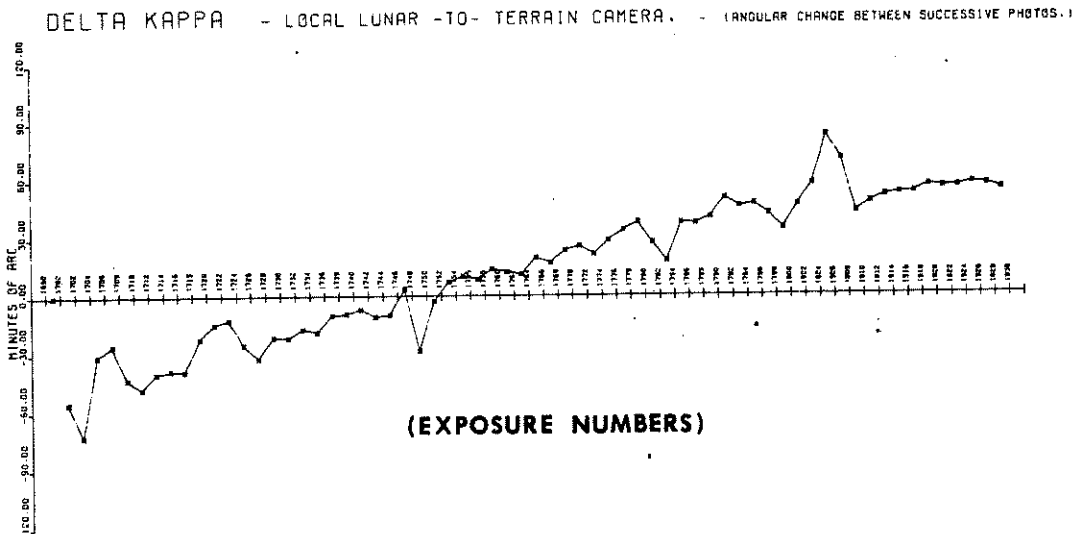
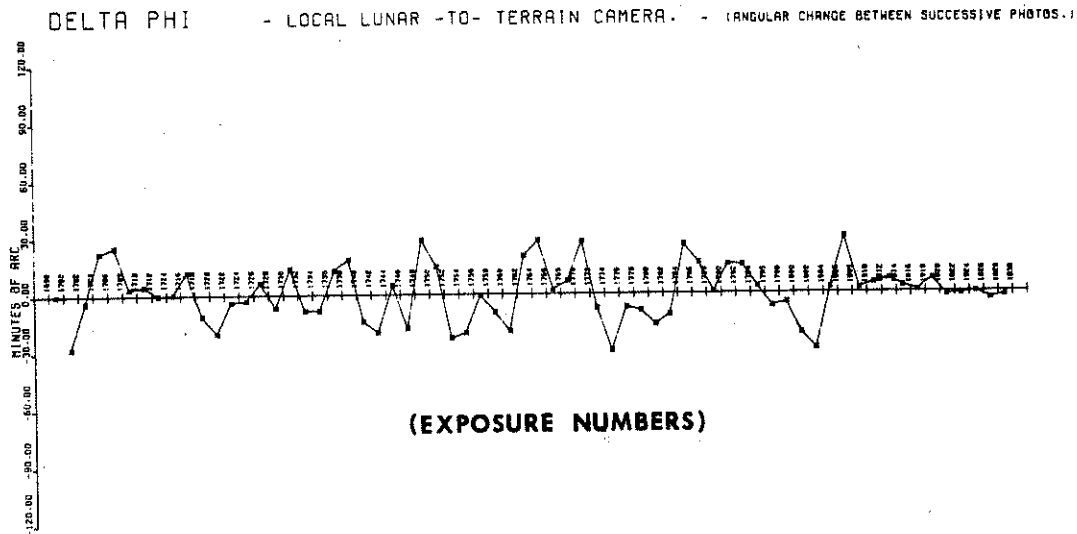
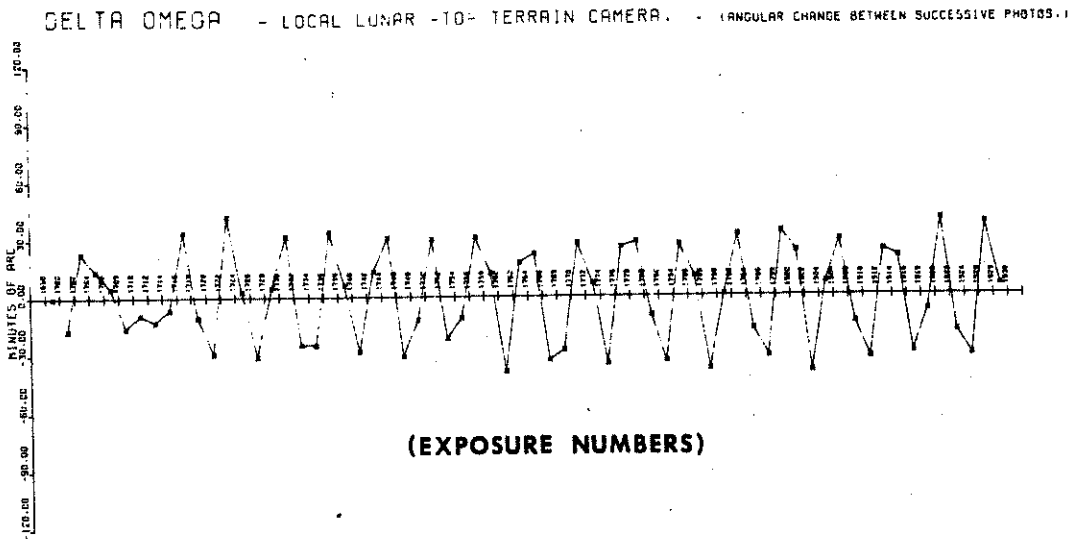


FIGURE 3.3 FIRST DIFFERENCES IN MAPPING CAMERA ORIENTATION ANGLES.



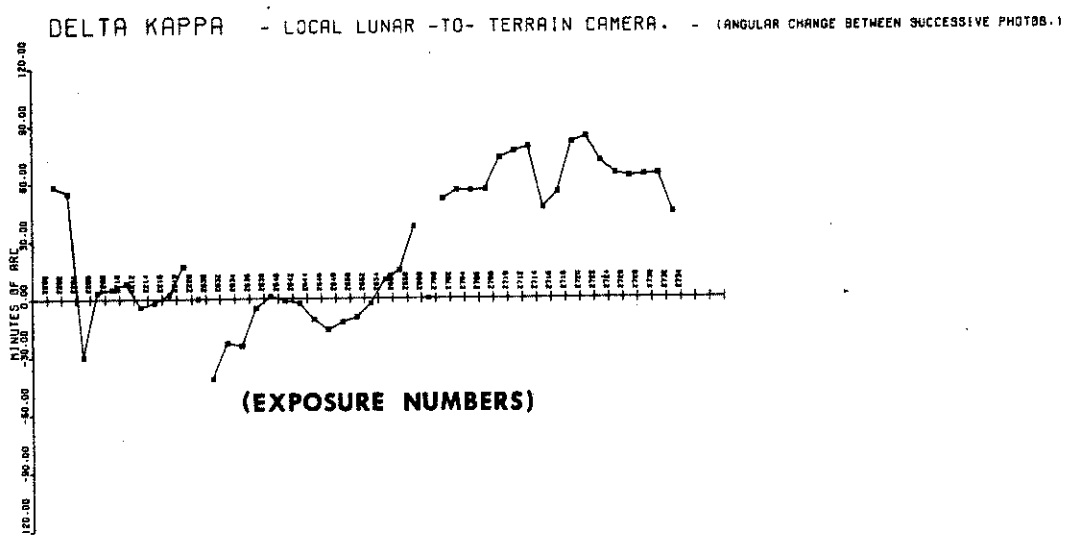
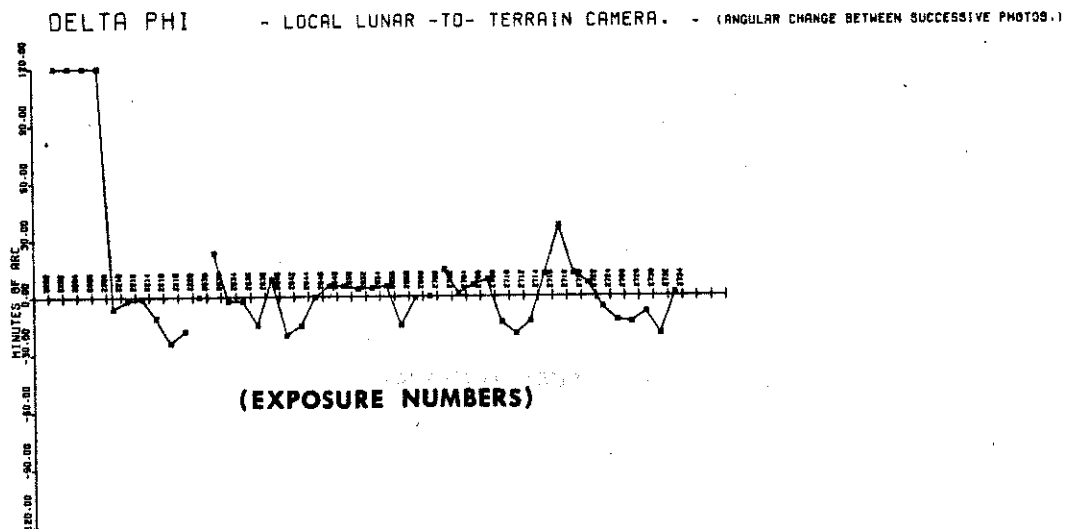
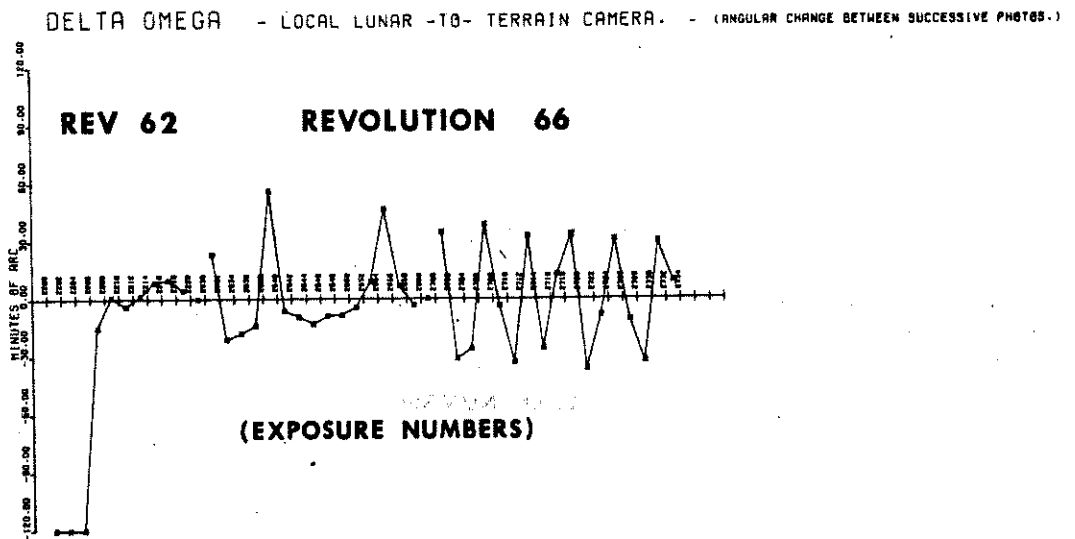


FIGURE 3.4 FIRST DIFFERENCES IN MAPPING CAMERA ORIENTATION ANGLES.

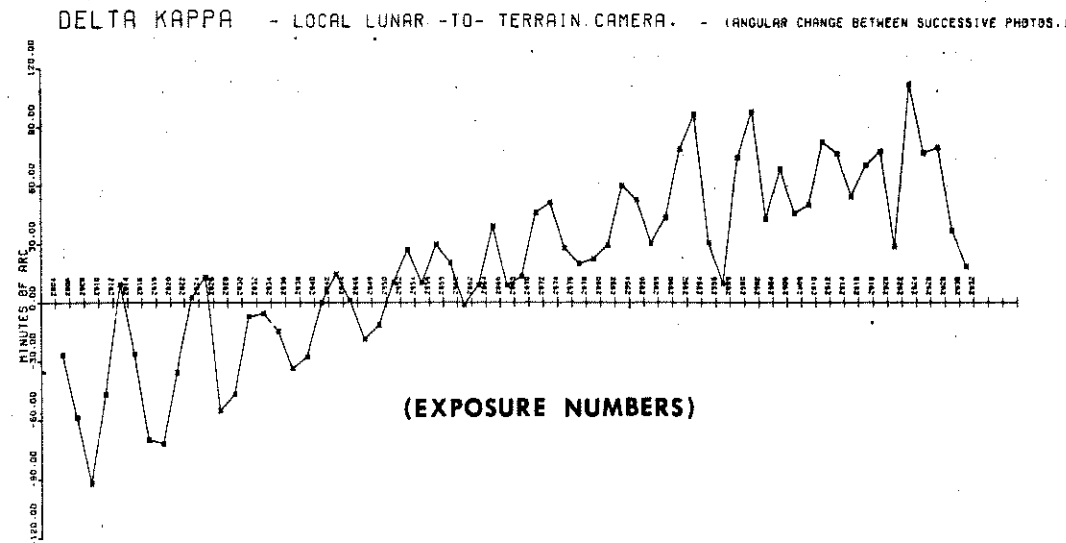
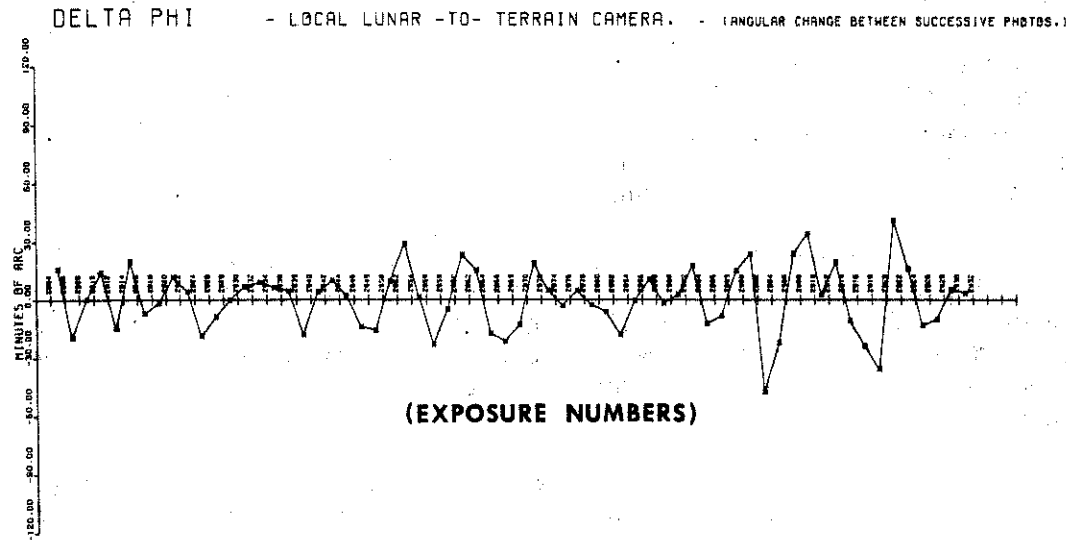
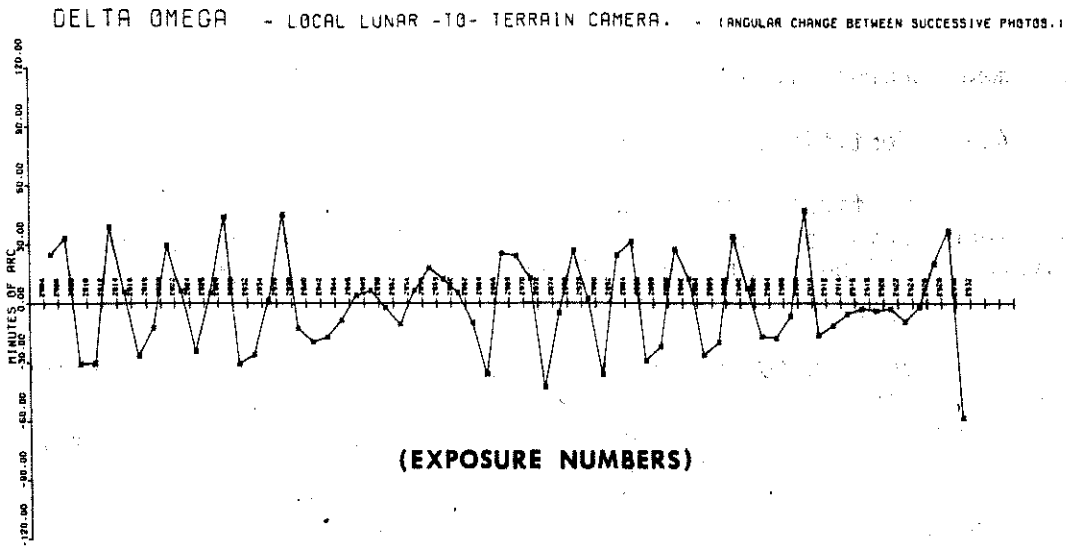


FIGURE 3.5 FIRST DIFFERENCES IN MAPPING CAMERA ORIENTATION ANGLES.

#### 4. Image Coordinate Acquisition and Reduction

##### 4.1 Identification and Mensuration

The first step of image coordinate identification was to select reference strips of photographs on which a basic pattern of lunar surface features could be identified. These strips were selected to provide maximum coverage of the lunar surface.

Lunar features were identified and marked on the photographs such that each photograph contained approximately 30 image points, where every other photograph was used. Where every photograph was used, each contained approximately 18 image points. The points were normally associated with the discrete images of small craters. The image points were marked using the Wild PUG II stereoscopic point transfer instrument. The features were observed stereoscopically on film positives enlarged two times and marked on one photograph of the stereo pair with a 30 micrometer drill. The marked image coordinates were transferred from the selected strips and measured on all corresponding photographs from sidelapping strips. In many cases the distribution of the images transferred to sidelapping strips was not geometrically acceptable and had to be supplemented by selecting and marking additional points.

The unique labeling scheme employed for the Apollo Mission 15, 16 vertical photograph reduction was expanded to incorporate the Apollo 17 exposures. This numbering system permitted the recovery of the photograph number on which any feature was originally selected, marked, and measured. The scheme of labeling and a description of the procedure is given in Appendix C.

Mensuration of the pass points was accomplished with the Nistri TA3/P stereocomparator using the enlarged film positives. A point was first monoscopically measured and recorded on the reference photograph, then stereoscopically transferred and measured on every corresponding exposure in the forward and sidelapping directions. The measuring procedure was repeated at least four times, twice in normal stereo and twice in pseudo-stereo (depth appears as height), and then monoscopic measurements were made of the four reseau intersections nearest the image measurement on each photograph. The stereo and pseudo-stereo readings were averaged to minimize reader bias. The removal of this bias produces a smaller standard deviation when the data is merged into a single solution.

## 4.2 Image Coordinate Reduction

### 4.2.1 Correction for Forward Motion Compensation

To compensate for the movement of the camera system relative to the lunar surface during the exposure sequence, a motion was imparted to the platen assembly (including reseau plate) and the film. Due to this motion, the relationship of the eight external fiducial marks to the internal reseau system was not constant from one photograph to the next. Therefore, it was necessary to determine the exact relationship of reseau to fiducials. The four nearest reseau intersections were used to correct the fiducials for film deformation in this case.

Second generation contact negatives were used to perform the measurements necessary to relate the reseau and fiducial systems. Each fiducial mark and the four nearest reseau intersections were measured monoscopically on the Nistri TA3/P stereocomparator. These measured coordinates were then input to the Lunar Coordinate Reduction (LCR) Program. This program corrected the measured coordinates of the fiducials for film deformation and adjusted them to the calibrated reseau system. The adjusted set of fiducial coordinates was then transformed to the calibrated fiducial system by means of a three parameter transformation.

The computed transformation parameters of the fiducial adjustment were examined for consistency in both the standard deviation and transformation coefficients. The standard deviations of the adjustments ranged from 2.4 to 7.5 micrometers. The few exposures which exhibited unexpected standard deviations or systematic photo residuals were re-measured and reprocessed as an edit of the initial results.

### 4.2.2 Correction for Systematic Errors

The LCR Program was used to correct and transform the comparator coordinates into the camera system. Input to the program consisted of the measured coordinates for all image points and their four nearest reseau intersections, camera calibration data, and the previously determined reseau to fiducial transformation parameters for each exposure. The program performed the following operations.

A. Sorted the measurement data and averaged multiple observations.

B. Transformed each image point into the photo coordinate system and corrected it for film distortion by adjusting the four nearest measured reseau coordinates to their respective calibrated values.

C. Transformed the corrected coordinates to the fiducial system by application of the transformation coefficients for the appropriate exposures.

D. Corrected all transformed image coordinates for principle point offset and radial and decentering distortions.

E. Output the final image coordinates on punch cards for input to the analytical triangulation programs.

#### 4.3 Altimeter Image Coordinates

A computer program was prepared for the Nistri TA3/PA automated stereocomparator to aid in the stereoscopic mensuration of the laser altimeter image coordinates. The LCR Program was modified during the Apollo 15 reduction to compute and output the calibrated photo coordinates of the altimeter point with respect to the reseau system. These coordinates were input to an online TA3/PA computer program before mensuration began. To measure altimeter coordinates the operator first measured from four to nine reseau intersections in the center of the photograph for the TA3/PA program to compute the comparator stage and reseau relationship. The stage was then automatically slewed to the computed "on line" altimeter image coordinates. The altimeter point was then measured stereoscopically by the same process used for measuring any image point. Although the altimeter points were not physically marked on the exposures, tests have shown that they can be recovered to within one or two micrometers by simply repeating the procedures.

Laser Altimeter Slant Range values were not recorded in the photo support data for the last 38 exposures in Revolution 2 or the first 18 exposures in Revolution 14. Observations of the altimeter position were not made on these exposures or on exposures where the recorded slant range value differed radically from those on adjoining exposures. An additional 56 altimeter observations were not included in the reduction due to the lack of detail at the point of measurement. These observations, however, were scattered throughout the reduction and represented a normal loss of data using this quality of imagery. Table 2 lists those exposures for which an Altimeter Slant Range was derived.

### 5. Analytical Triangulation

#### 5.1 Strip Relative Solutions

Each strip or subsection of a strip was analytically triangulated with the Relative Analytical Block Orientation (RABO) (4) Program. Input

TABLE 2

EXPOSURES WITH DERIVED ALTIMETER SLANT RANGE

<u>Revolution</u>	<u>Exposure</u>
2	172,176-180 181-218,220-229*
14	346-354,358 362-380,394 398-422
29	1386-1392,1396 1400-1416 1442-1448,1452,1454 1458,1464-1480
38	1694,1696,1700,1704 1706,1710-1716,1720 1726,1730,1734-1738 1744,1750-1760 1764-1776,1780-1798 1802-1818,1821,1822 1824,1825,1826
49	2031-2034,2036-2050*
62	2200-2212,2216-2220
66	2630-2644,2648-2660 2700-2730
74	2796,2798,2804-2828 2832-2850,2854-2902 2902-2932

Even numbered exposures were used unless noted  
\* Every exposure used

to the RABO consisted of the corrected image coordinates of surface features and altimeter locations, the camera position for each exposure, and the stellar derived orientation angles. The lunar-fixed selenocentric position vectors and orientation angles obtained from SATLUM were input to the RABO in the Universal Space Rectangular (USR) System. These strip RABO solutions were used as a quality control edit to detect image measurement blunders and to provide an estimate of the average mensuration accuracy for the image coordinates. The standard deviations of the image measurement residuals from these solutions ranged from 3.1  $\mu\text{m}$  to 6.0  $\mu\text{m}$ . In general, the lower standard deviations were associated with photographs which did not have a very low or very high sun angle.

## 5.2 Strip Constrained Solutions

The Simultaneous Adjustment of Photogrammetric and Geodetic Observations (SAPGO) (5) Program was used to compute an initial solution with the photographs of each revolution. This conventional triangulation program has the capability to simultaneously reduce photographic image coordinates, exposure station positions, orientation angles, and the object space coordinates for strips or blocks of photographs according to their apriori constraints.

The lunar fixed orientation angles obtained from SATLUM were constrained to 30 seconds of arc in each component. Lunar-fixed orientation angles were obtained from the photo support data for the terrain exposures that did not have useable companion stellar exposures. These orientations were constrained to 5 degrees of arc in each component. The exposure station positions were constrained to 200 meters in X, Y, and Z (USR) and the altimeter values were constrained to 50 meters. The image coordinate standard deviation was held to 7 micrometers based on examination of the RABO solutions.

Figures 4, 4.1, and 4.2 display the horizontal and vertical adjustments made to the initial camera positions in the strip SAPGO solutions for three sample revolutions. The revolutions shown (14, 38, and 74) are representative of the changes made to ephemeris positions. Figure 4.2 shows the corrections for every photograph in strips 14 and 74. Examination of the exposure station changes in the plots of the individual strip solutions indicated two things: first, that periodic type discrepancies appear in the ephemeris positions; and second, the solution for strip 74 shows the most consistency among all input data types.

Comparisons of selenographic coordinates of the same lunar features derived independently in two or more SAPGO strip solutions were

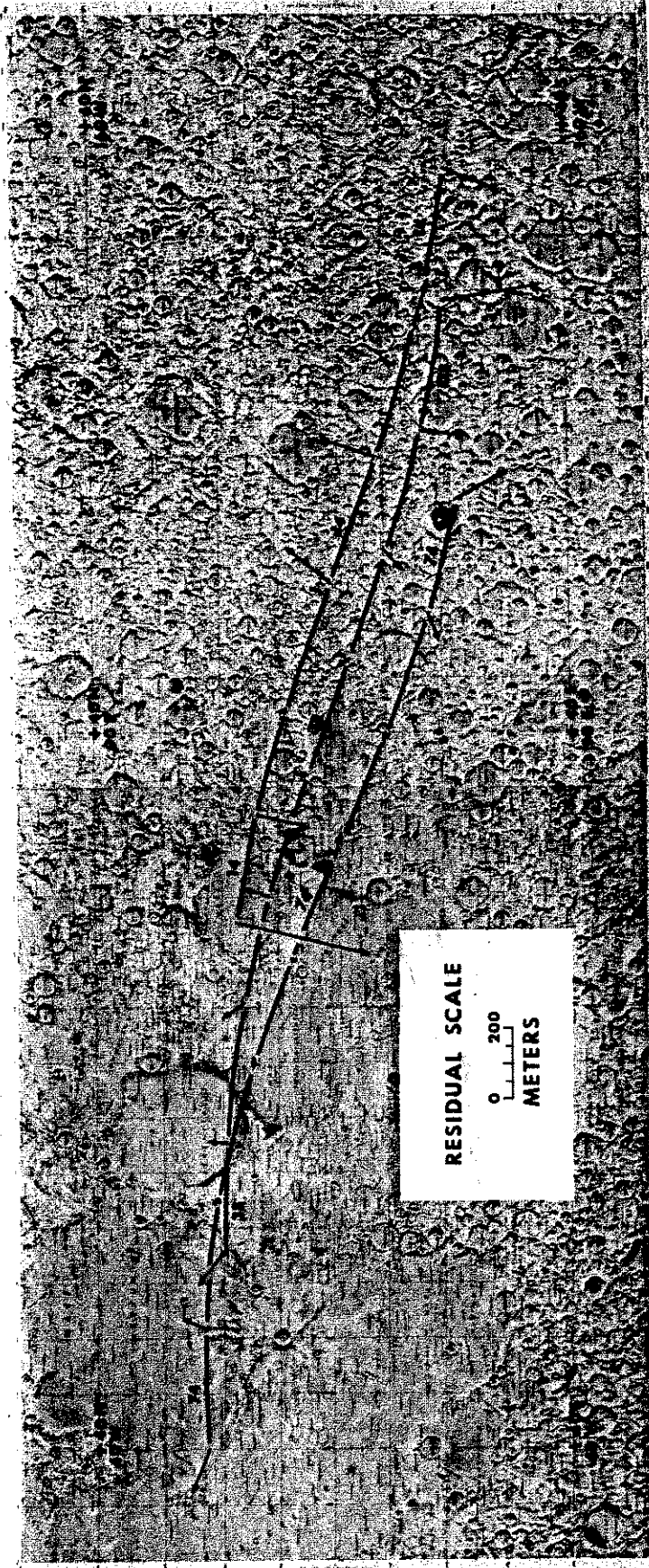


FIGURE 4. HORIZONTAL ADJUSTMENT OF STRIP SARGO SOLUTION.



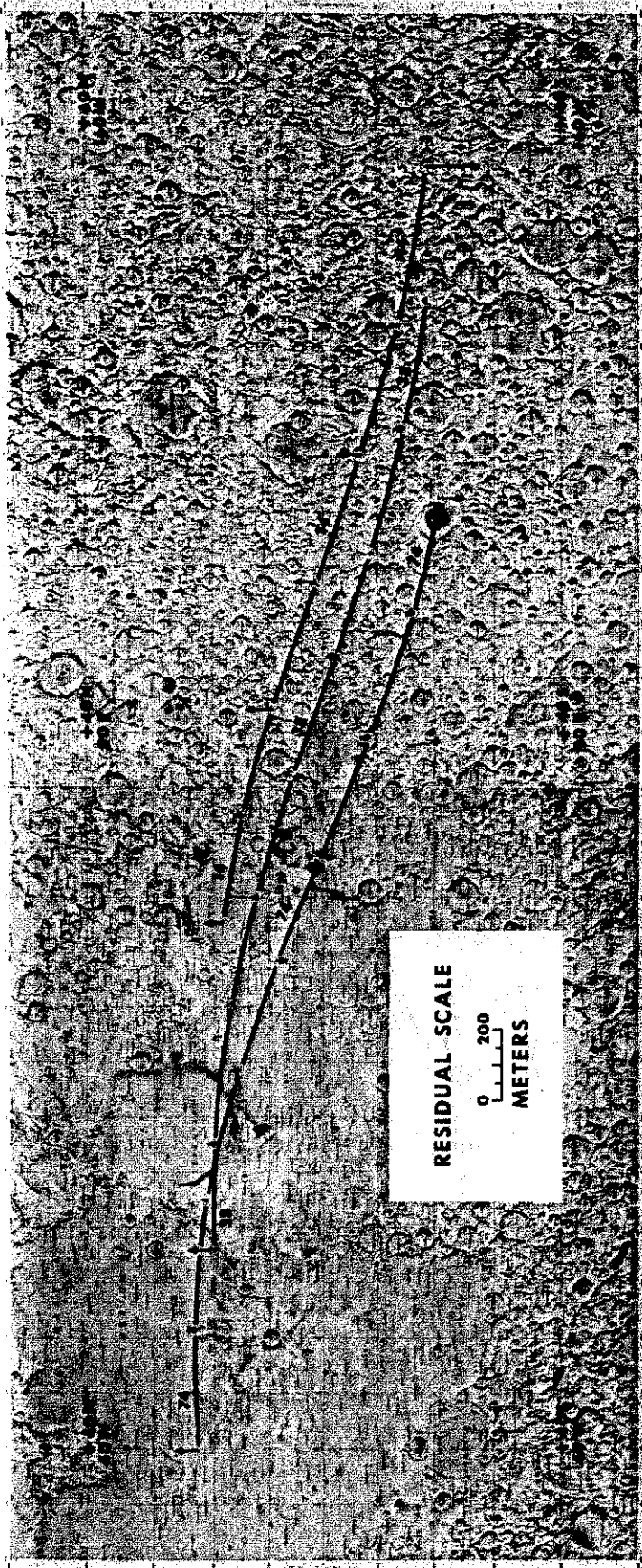
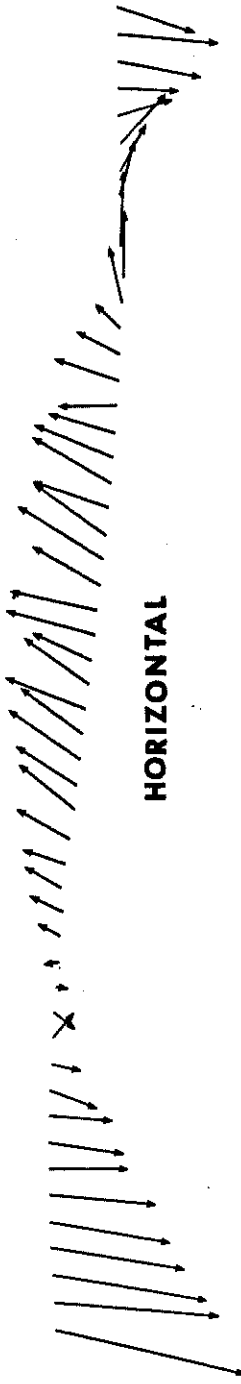
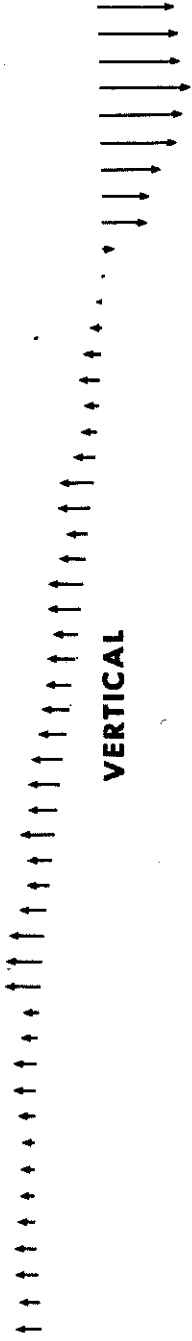


FIGURE 4.1 VERTICAL ADJUSTMENT OF STRIP SAPGO SOLUTION.

REV 14

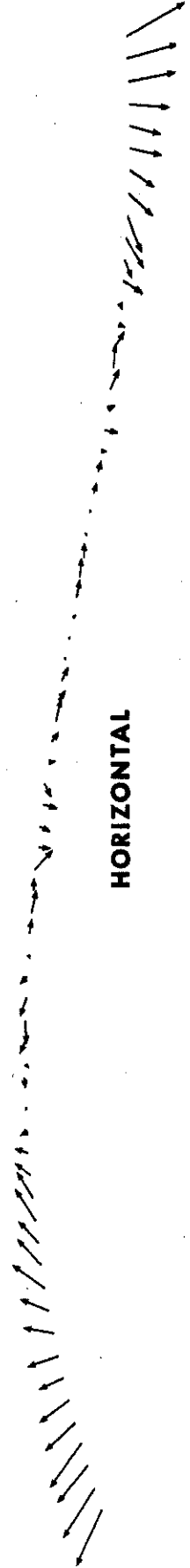


HORIZONTAL

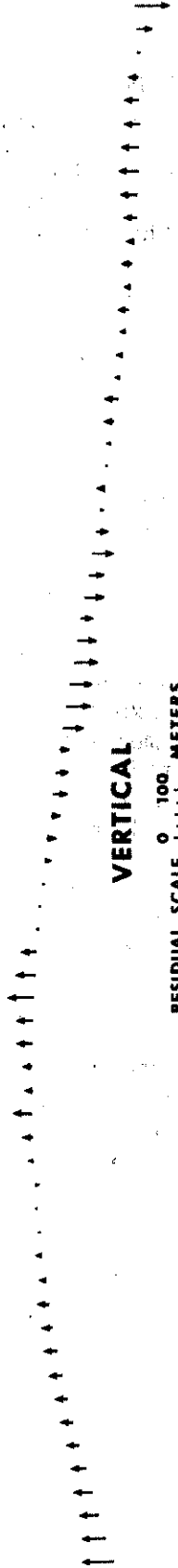


VERTICAL

REV 74



HORIZONTAL



VERTICAL

RESIDUAL SCALE 0 100 METERS

OBLIQUE MERCATOR PROJECTION

FIGURE 4.2 HORIZONTAL AND VERTICAL ADJUSTMENTS OF STRIP SAPGO SOLUTIONS.

made. In this analysis the mean systematic positional bias between the common points of sidelapping strips was computed. The selenographic coordinates derived from one revolution were selected as a standard and the coordinates from a sidelapping revolution were then compared to those of the standard. Table 3 shows the systematic biases between revolutions. It is evident that the greatest overall variations usually occur in the latitude component which generally represents a discrepancy in the cross-track component of the ephemeris. The in-track and radial components (approximately the same as longitude and height) compare more favorably.

Analysis of the differences of common points between strips (with the mean systematic biases removed) indicated that non-linear discrepancies no longer existed over the length of the strip solutions. This result supported the assumption that the periodic discrepancies of the triangulation parameters were caused by the ephemeris positions. By enforcing the photogrammetric conditions, relatively consistent surface coordinates were produced.

### 5.3 Block Triangulation Solution

The SAPGO computer program was also utilized for the block triangulation solution. The present program data storage capabilities of 700 exposures and 6,000 surface coordinates were commensurate with the requirements for the total block solution. The program in this case performed a simultaneous solution with essentially the same data set found in the strip SAPGO solutions. All the exposures used in the strips were used in the block.

From the analysis of the strip SAPGO solutions the following decisions were made for further data reduction work. First, revolutions 38, 62 and 74 were selected to provide the absolute positional datum for the total Apollo 17 block reduction. The reasons for making this choice were (1) the solution indicated that the input parameters were more compatible for these strips than the others (2) comparisons of common points showed that these revolutions approximated the mean position of the strips in the block. Next, the ephemeris camera positions for all revolutions would be allowed to adjust in the solutions in order to achieve compatibility with image measurements and attitude information. Lastly, altimeter measurements of the camera station positions would be constrained to achieve the best possible fit to the ephemeris, at least to the extent that the apriori constraints of the other parameters are not violated.

TABLE 3

MEAN SYSTEMATIC BIASES BETWEEN COMMON SURFACE COORDINATES  
 DERIVED IN INDEPENDENT STRIP SAPGO SOLUTIONS

<u>Standard Revolution</u>	<u>Comparison Revolution</u>	<u>Number of Common Coordinates</u>	<u>Latitude</u>	<u>Mean Biases (Meters) Longitude</u>	<u>Height</u>
2	14	303	49	60	-54
2	29	30	408	-31	-155
29	14	128	-618	104	270
29	38	245	-243	189	-187
29	49	21	218	-157	-70
38	14	30	-333	-213	370
38	49	82	454	-125	183
38	62	9	74	-56	-64
38	66	17	-104	-54	68
62	49	19	321	-23	370
66	62	54	-79	103	-118
74	2	12	-736	555	113
74	38	54	-160	-38	-32
74	62	15	-16	-104	-127
74	66 1st Part	62	39	-209	-38
74	66 2nd Part	110	-290	-60	83

The positional constraints assigned to X, Y, Z, (USR) components were as follows:

<u>Revolution</u>	<u>Constraint in Meters</u>
2	1000
14	500
29	300
38	100
49 (partial)	500
62 (partial)	100
66 (partial)	200
74	100

The constraints placed on the angular orientations derived from the SATLUM Program were 30" of arc, while those obtained from the ephemeris (for terrain exposures without companion stellar exposures) were 5° of arc. An average standard deviation of 8 micrometers was selected as representative of the reliability of the image measurements in the block. This value approximates a combination of within-strip and cross-strip identification and mensuration accuracy. The altimeter slant range values were held to 50 meters.

Analysis of the first block solution brought about the following changes. The camera position constraints would be applied in a local system in order to provide an altitude constraint for each revolution. The horizontal (x, y) constraints remained the same except for Revolution 2 which was changed to 1500 meters and Revolution 66 which was changed to 100 meters. The vertical constraint (z) remained the same for Revolutions 14 and 38, but was changed on Revolutions 2, 29, 49, 62, 66 and 74 to 1500, 225, 200, 150, 75 and 75 meters respectively.

In the final simultaneous block SAPGO solution, the standard deviation of the image-measurement residuals was computed to be 6.6 micrometers. Changes to the orientation parameters were well within the a priori constraints. Figures 5 and 5.1 illustrate the horizontal and vertical changes in the camera positions. The solution computed selenographic coordinates for 3945 lunar features and adjusted exterior orientation parameters (positions and attitudes) for the 408 photographs in the solution. Of the 3945 feature positions reduced 889 were common to the Apollo Mission 15 reduction. Figure 6 shows the area of common vertical photographic coverage between Apollo Mission 15 and Apollo Mission 17.

One goal of the block SAPGO analysis was to check the validity of the corrections made to the exterior orientation parameters of each photograph. In order to do this the adjusted exposure station and orientation parameters were used with the image measurements of each revolution to independently derive selenographic coordinates for common surface features. The RABO Program was used for this purpose by

NATIONAL AERONAUTICS AND SPACE ADMINISTRATION  
LUNAR CHART

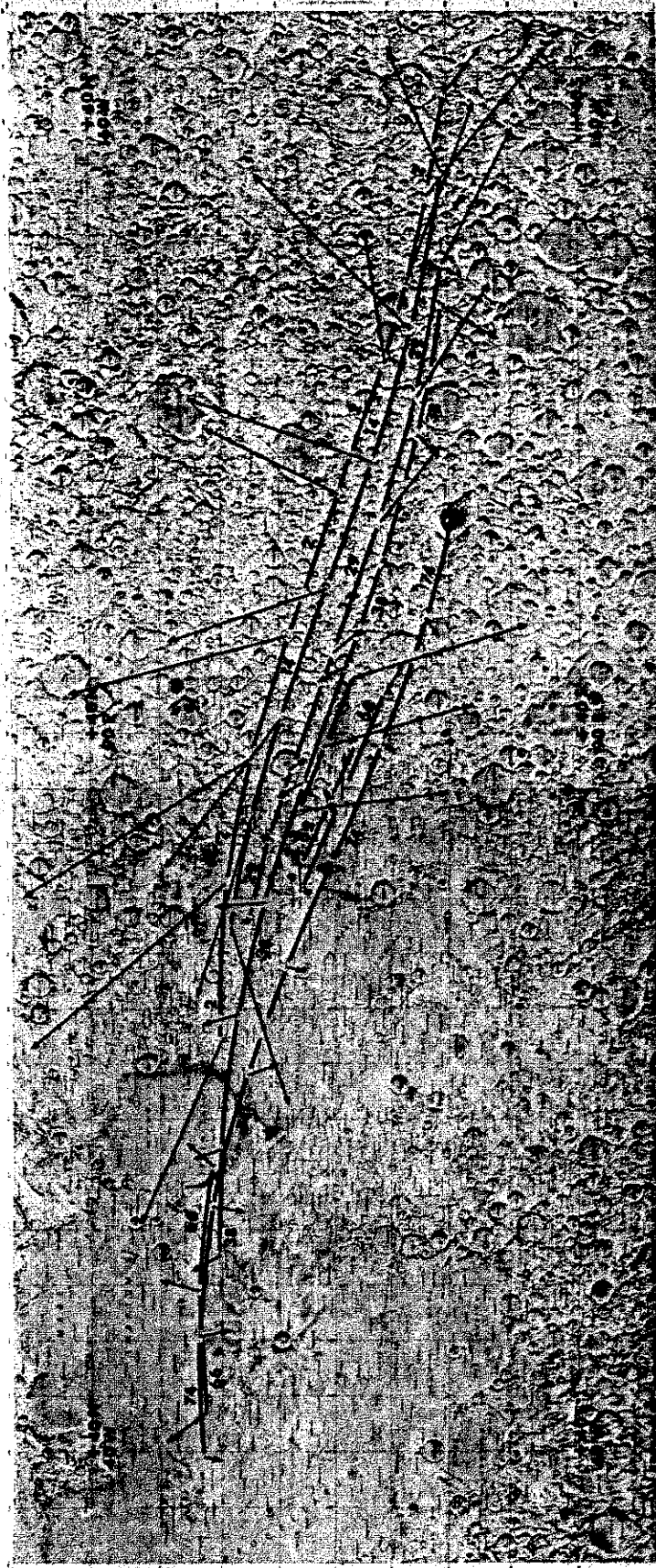
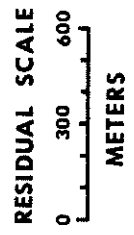


FIGURE 5. HORIZONTAL CHANGE TO CAMERA POSITIONS FINAL BLOCK SOLUTION.



NATIONAL AERONAUTICS AND SPACE ADMINISTRATION  
LUNAR CHART

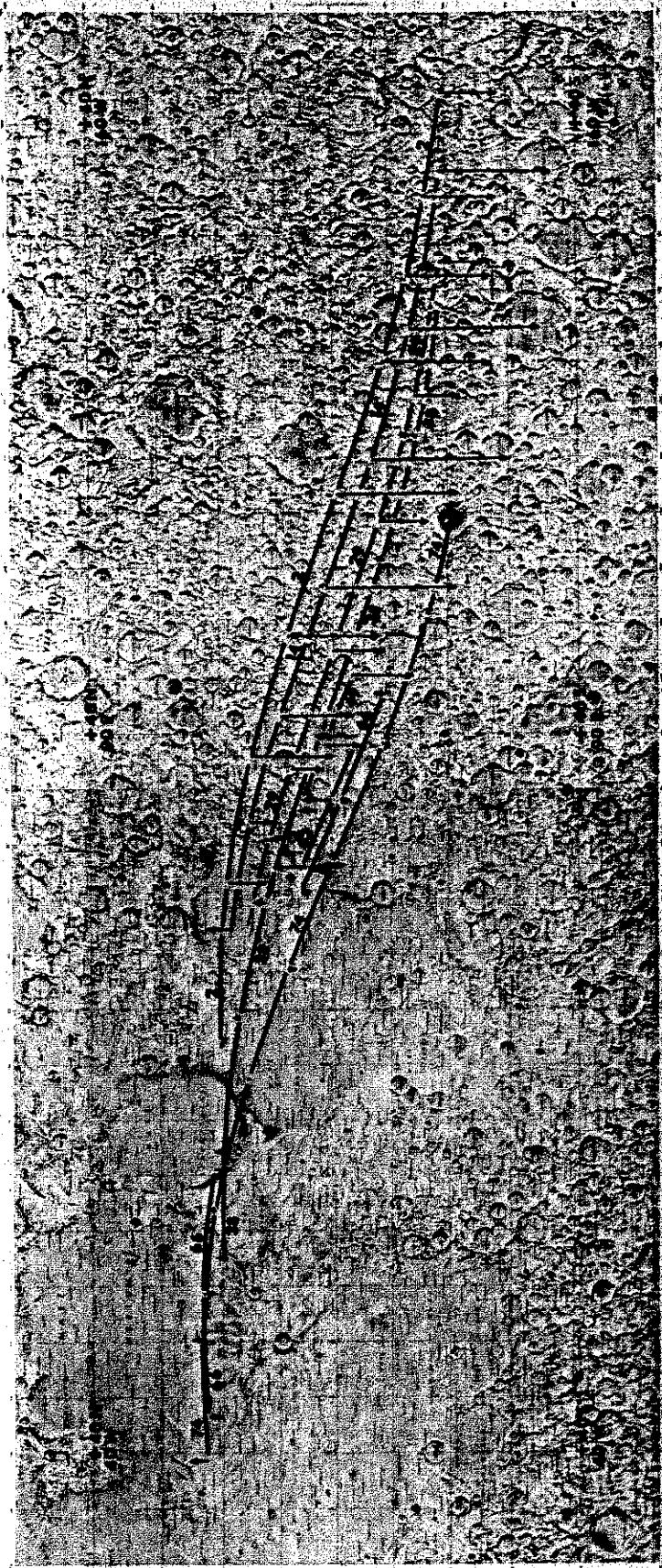
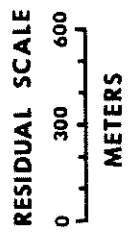


FIGURE 5.1 VERTICAL CHANGE TO CAMERA POSITIONS FINAL BLOCK SOLUTION.





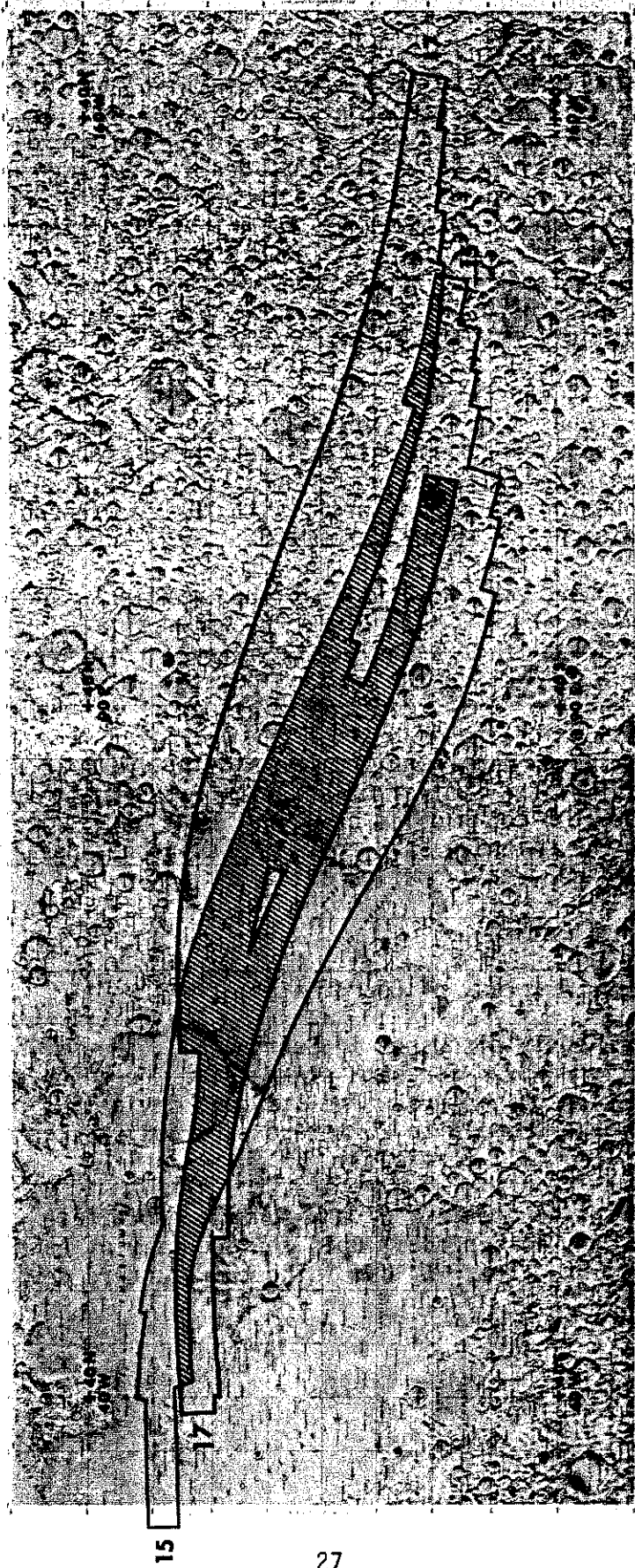


FIGURE 6. COMMON VERTICAL PHOTOGRAPHIC COVERAGE BETWEEN APOLLO MISSIONS 15 AND 17.



exercising the option which computes a rigorous intersection solution. Thus, for a feature measured on the photographs of two overlapping revolutions two sets of selenographic coordinates were available, one set from each revolution with each set based on the corrected exposure parameters for its revolution. The RABO derived selenographic coordinates for all pass points measured on more than one revolution were compared in this fashion. A computer program was used to calculate the positional difference between common points, to generate the plots that graphically portrayed these differences, and to compute the standard deviations of the differences in each component (latitude, longitude, and height). Table 4 shows the statistical results of these comparisons.

The plots generated by the program were carefully examined for any systematic trends in the residuals. No systematism was noted and the computed averages for each data set were near zero. The results of the analysis indicated that the positional relativity achieved in the block SAPGO reduction was commensurate with that projected from the assumed accuracies of the input parameters.

It is noted that Revolution 62 had marginal sidelap geometry with Revolutions 38 and 49. There were 6 common surface points used on Revolutions 62 and 38 to establish positional relativity in the reduction. There were 19 common surface points measured on both Revolutions 62 and 49. This resulted in a span of eleven exposures on Revolution 62 for which the adjusted block parameters represent an extrapolation based on a marginal common sidelap, with geometrical constraints added by the stellar orientation data and the positional constraint. Although the problem could not be avoided, it should be recognized that the selenographic coordinates in this area result from a less than ideal geometric configuration.

## 6. Positional Evaluation

### 6.1 Relative Accuracy of Coordinates

As previously discussed in Section 5.3, the surface positions were independently derived for each strip using the adjusted block exterior orientation parameters. The standard deviations presented in Table 4 give a range from 16 to 25 meters (CE, 39%) horizontally and from 14 to 26 meters (LE, 68%) vertically.

The relative accuracy of any surface coordinate with respect to another, however, is dependent upon the accuracy of each point relative to the triangulation datum. By combining the standard deviations between

TABLE 4

STANDARD DEVIATIONS COMPUTED FROM COMPARISONS  
OF COORDINATES COMMON TO TWO OR MORE STRIPS

Standard Revolution	Comparison Revolution	Common Coordinates	Standard Deviations (Meters)			
			Lat (68%)	Long (68%)	Horizontal CE(39%)	Vertical LE(68%)
2	14	239	25	17	21	26
29	2	23	22	18	20	21
29	14	123	18	15	17	21
29	38	212	20	15	18	22
29	49	13	26	21	24	18
38	2	58	27	19	23	24
38	14	23	21	17	19	20
38	49	69	30	18	25	25
38	62	6	25	21	25	24
38	66 2nd Part	9	14	20	17	20
62	49	15	20	19	20	22
66	62	50	24	19	21	18
74	2	9	31	19	25	18
74	38	47	19	18	19	14
74	62	11	31	17	25	17
74	66 1st Part	50	22	17	20	24
74	66 2nd Part	105	18	13	16	15

revolutions an estimate of this point to point accuracy can be determined. Using the standard deviations presented in Table 4 the estimated average circular relative standard error is 21 meters (CE, 39%) and the mean vertical error is 21 meters (LE, 68%).

The Apollo 17 derived datum may be related to the true datum by seven parameters (one for scale, three for orientation, and three for translation). An error in scale or orientation will contribute to the relative error between surface coordinates. This may be written in simplified form as:

$$\sigma_T^2 = \sigma_i^2 + \sigma_j^2 + \sigma_p^2 \quad (6.1)$$

where  $\sigma_T^2$  is the relative variance between the two points,  
 $\sigma_i^2$  and  $\sigma_j^2$  are the variances relative to the Apollo 17 reduction, and  
 $\sigma_p^2$  is the variance of scale and orientation.

The i and j are assumed equal and uncorrelated therefore:

$$\sigma_T^2 = 2\sigma_i^2 + \sigma_p^2 \quad (6.2)$$

One other condition was imposed in equation 6.2 to account for the condition that  $\sigma_p^2$  is a function of the distance between the coordinates being evaluated. The estimated effect of this condition is introduced by modifying equation 6.2 to:

$$\sigma_T^2 = 2\sigma_i^2 + \left(\frac{d}{D} \sigma_p\right)^2 \quad (6.3)$$

where d is the actual distance between the two coordinates, and

D is the total distance covered by the triangulation (7400 km).

To obtain some appreciation for this estimate of accuracy between coordinates, computations were made using equation 6.3 and varying the distance (d) between coordinates. The values used for  $\sigma_p^2$  were the assumed standard deviations of 100 meters horizontally and 75 meters vertically for Revolutions 66 and 74 in the block triangulation.

The values used for  $\sigma_1^2$  were the circular and vertical accuracies estimated for the block solution. Table 5 gives the results of the computations.

## 6.2 Relative Position of Apollo Mission 17 and Apollo Mission 15 Solutions

The 889 points common to both the Apollo Mission 17 reduction and the Apollo Mission 15 reduction were compared by determining the mean distance from the Apollo 15 point positioning to the Apollo 17 positions. The Apollo 17 positions derive approximately 600 meters to the Northeast of the Apollo 15 positions except for the western end which derive East of the Apollo 15 positions. The change in azimuth is attributed to the lack of laser altimeter constraints for the Apollo 15 in this area. The vertical differences vary with Apollo 17 being 200 meters lower than Apollo 15 at the eastern end - zero at the center - and 200 meters higher at the western end. Figures 7 and 7.1 illustrate the change for every tenth point.

## 6.3 Laser Altimeter Slant Range Derivation

The mean difference between the derived altimeter distances and the photo support data is +10 meters. Of the 291 altimeter points used in the block solution 17 exceeded the 50 meter constraint. The largest of these was 89 meters. These points were retained even though the photographic imagery was marginal. Ninety percent of the derived altimeter slant range distances varied less than 40 meters from their computed value.

## 6.4 Absolute Positional Evaluation

The absolute positional evaluation for any coordinate derived from the block reduction with respect to principal axes of inertia and the center of mass of the moon would be a combination of the relative accuracy of the coordinate with respect to the datum (Section 6) and the accuracy of the datum in an absolute sense. The relative accuracy strip to strip has been discussed above; however, the absolute accuracy of the Apollo 17 datum can only be estimated at this time. Analysis of the discrepancies between strip solutions given in Section 5.2 would yield an average bias of approximately 260 meters. These biases may be used as an indication of the accuracy of the Apollo 17 spacecraft ephemeris. Because of discrepancies that are found in inter-orbit comparisons of the ephemeris, no absolute evaluation is determined at this time.

**TABLE 5**

**ESTIMATED RELATIVE ACCURACY BETWEEN  
POINTS SEPARATED BY VARIOUS DISTANCES**

<u>Distance Between Points (KM)</u>	<u>Point to Point Relative Accuracy (M)</u>	
	<u>Horizontal (39%)</u>	<u>Vertical (68%)</u>
0	30	30
1000	36	31
3000	65	42
5000	100	58
7000	137	76
7400	144	80

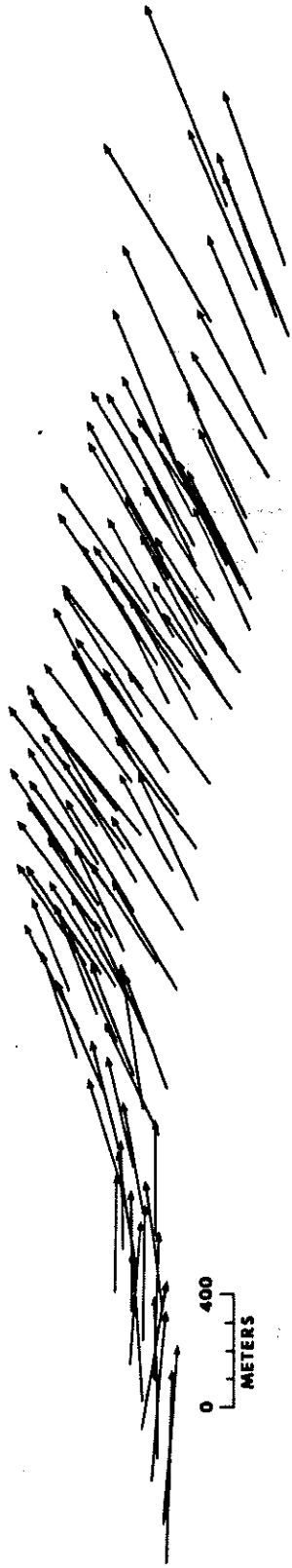


FIGURE 7. HORIZONTAL POSITION COMPARISON OF APOLLO 17 TO THE APOLLO 15 BLOCK SOLUTION.

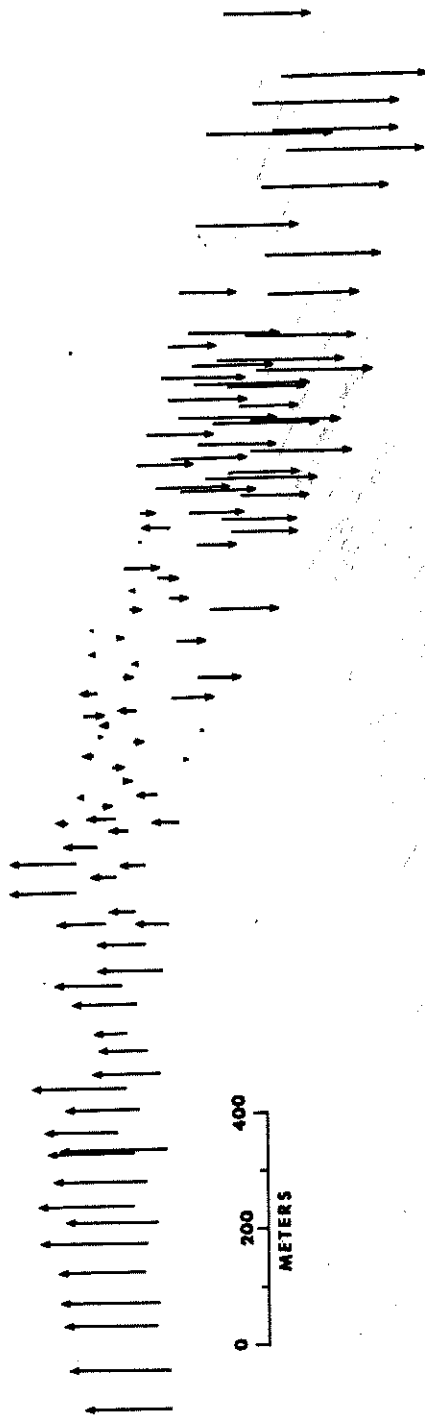


FIGURE 7.1 VERTICAL POSITION COMPARISON OF APOLLO 17 TO THE APOLLO 15 BLOCK SOLUTION.

## 7. Generated Products

The following items have been produced as a result of the Apollo 17 data reduction assignment.

7.1 Composite film negatives annotated and marked to provide photo identifications for recoverable pass points.

7.2 Magnetic tapes containing the following input and output parameters.

7.2.1 The transformation coefficients ( $X_0$ ,  $Y_0$ ,  $\alpha$ ) that were used to relate the reseau system to the fiducial system for each mapping exposure.

7.2.2 Image measurements in the photo coordinate system for all 408 mapping exposures.

7.2.3 The USR orientation angles of the mapping exposures as determined in the stellar reduction processes.

7.2.4 The USR positions for all exposures as obtained from the photo support data.

7.2.5 The adjusted USR exposure station position and orientation for each exposure included in the block reduction. The orientations are given in both matrix and angular form.

7.2.6 The output selenographic and USR coordinates for all pass points as derived in the block reduction.

7.2.7 Laser altimetry information for all exposures in the block solution that had recorded altimeter observations. The following information is available for each exposure.

7.2.7.1 The revolution and exposure number.

7.2.7.2 The x and y photo coordinate of the altimeter point in millimeters.

7.2.7.3 The observed slant range in kilometers.

7.2.7.4 The slant range, in kilometers, as computed using the adjusted parameters from the block reduction.



## 8. Conclusions

From the analysis of the results of the total Apollo 17 reduction, the following conclusions have been reached.

8.1 The accuracies of photogrammetrically derived data agree favorably with the estimates determined in the initial testing of the Apollo 17 photography.

8.2 The standard deviations computed in SATLUM were improved as a result of the revised Apollo Mission 17 camera calibration.

8.3 Changes within strip and between strip camera station positions observed in the reduction of Apollo 17 can be correlated to the Apollo 17 ephemeris.

8.4 Altimeter point image coordinates provide a consistent data set which should be mathematically introduced into the analytical triangulation solution.

8.5 The accuracy of selenographic coordinates relative to the datum established by the triangulation solution are commensurate with the accuracies of the input data. They meet the accuracy objective of the original DMAAC data reduction proposal.

8.6 Coordination should take place between all investigations which potentially could improve the absolute relationship of the Apollo 17 datum to the axes of inertia and center of mass of the moon.

## REFERENCES

1. Apollo 17 Metric System Initial Evaluation Report, Defense Mapping Agency, Aerospace Center, April 1974.
2. Final Technical Report, Computer Program for Utilization of Stellar Photography for Determining the Attitude of a Terrain Camera in a Local Lunar Coordinate System, Raytheon Company, March 1971.
3. Camera Calibration Report Apollo Mission 17, Lunar Mapping Camera Unit SN-004, Defense Mapping Agency Aerospace Center, June 1974.
4. Apollo 15 Initial Metric System Evaluation Report, Aeronautical Chart and Information Center, March 1972.
5. Simultaneous Adjustment of Photogrammetric and Geodetic Observations, Wong, K. W. and Elphinstone, G. M., Presented Paper, ASP Annual Meeting, Washington, D. C., March 1971.
6. Camera Calibration Report, Camera Unit SN-004, Fairchild Space and Defense Systems, August 1971.
7. Advance Methods for the Calibration of Metric Cameras, D. Brown Associates Inc., for U. S. Army Engineering Test Laboratories, December 1968.
8. Principles of Error Theory and Cartographic Applications, Aeronautical Chart and Information Center, Technical Report No. 96, St. Louis, Missouri, February 1962.
9. Development of the Apollo 15 Control Network, Defense Mapping Agency, Aerospace Center, August 1973.
10. Apollo 15 Stellar Reduction, Cannell, W. and Doepke, L., Annual Meeting, American Society of Photogrammetry, March 1973.
11. Selenodetic Control Derived from Apollo Metric Photography, Helmering, R. Lunar Science Institute Conference, January 1973.
12. Lunar Shape Via the Laser Altimeter, Sjogren, W. L., and Wollenhaupt, W., Science, January 1973.